A STUDY OF THIN FILM VACUUM DEPOSITED JUNCTIONS

Semiannual Status Report

on

NASA Grant NsG-340

Submitted by:

Dr. Robert L. Ramey

Professor of Electrical Engineering

Research Laboratories for the Engineering Sciences

University of Virginia

Charlottesville

Report No. EE-4012-106-66U

June 1966

A STUDY OF THIN FILM VACUUM DEPOSITED JUNCTIONS

Semiannual Status Report
on
NASA Grant NsG-340

Submitted by:
Dr. Robert L. Ramey
Professor of Electrical Engineering

Division of Electrical Engineering
RESEARCH LABORATORIES FOR THE ENGINEERING SCIENCES
SCHOOL OF ENGINEERING AND APPLIED SCIENCE
UNIVERSITY OF VIRGINIA
CHARLOTTESVILLE, VIRGINIA

Report No. EE-4012-106-66U
June 1966 Copy No. 4

TABLE OF CONTENTS

LIST OF FIGURES

SECTION I
REPORT COVERAGE

This semiannual report covers the period from December 5, 1965 to June 5, 1966. This research program is currently in its fourth year of operation.

SECTION II
STATUS OF RESEARCH

Theoretical and analytical research on the effects of surface and body states upon the carrier concentration and mobility in thin films has been completed. The results are currently being applied to experimental data and the conclusions along with the theory will be reported in the next annual status report (December 5, 1966).

In the Semiannual Status Report (No. EE-4012-104-65U) for June 1965 it was mentioned that we were initiating an investigation into electron tunneling devices where the electrode films were atomically rough. For instance, a rough cathode surface should result in a tunnel sandwich structure with unilateral properties. Our original suggestion was the use of metallic whiskers, grown upon the cathode, to produce the desired surface conditions. As a result of our work on this problem during the past year, we have developed a model for any electron tunneling device based upon electrodes which are rough in terms of atomic lattice dimensions. The theoretical and experimental results of this investigation are included in Section III. It is anticipated that this approach to the general problem of analyzing electron tunneling experiments will point the way to successful device design. The material of Section III has been submitted to the Journal of Applied Physics for publication.

SECTION III
EFFECTIVE THICKNESS AND HEIGHT OF THE BARRIER FOR CHARGE TRANSPORT THROUGH ATOMICALLY ROUGH FILMS

It has been suggested by many authors that if two electrodes are separated by sufficiently thin insulating films the predominant electron transfer mechanism is due to the quantum-mechanical process of tunneling. This was first considered by Frenkel [1] in 1930 when he derived expressions relating tunneling current and voltage by considering a rectangular potential barrier for the insulating gap and using the electron free mass in both the metals and the insulator. Sommerfeld and Bethe [2] were able to extend his work and establish mathematical expressions which were applicable to very low and very high voltage cases. Holm [3] extended the theory to include the intermediate voltage range; however, certain anomalies which appeared in his work were later corrected by Simmons [4].

This phenomenon of electron tunneling has received considerable attention in recent years because of the possibility of designing electronic devices for amplification and as transducers which rely upon this method of transport in their operation. It was the purpose of this phase of our research to investigate electron tunneling in thin film structures and to derive a method of determining the metal-insulator work function and effective film thickness.

Theoretical expressions for the electron tunneling current density and the Schottky enhanced current density through thin insulating films form a set of transcendental equations in terms of the effective barrier thickness and height. From measured volt-ampere-temperature characteristics important thin film structure parameters can be calculated.

In insulating films between two metal contacts there are three general mechanisms which may establish an electric current. These are Schottky emission, space charge limited current, and direct electron

tunneling. Since space charge limited current applies to rather thick dielectric films with ohmic contacts, it was of no importance to this investigation.

The action of the insulating material between the two metal electrodes is to introduce a potential barrier which impedes the flow of electrons. If this insulating barrier is sufficiently thin there is a significant probability that an electron be transmitted directly through this region by electron tunneling.

It is common practice to consider plane parallel electrodes separated by a uniform insulating film as representing the typical experimental film structural arrangement (Figure 1A). The actual film is probably far from the ideal structure, however, with both film surfaces being irregular as shown in Figure 1B. For this nonideal film the regions of close electrode approach, where the insulating film is thin, may be described in terms of a total effective surface area and a mean effective thickness although this will introduce an effective surface area which may be only a small fraction of the gross geometrical area of the structure. It will be assumed that this effective electrode area can be interpreted by the concept of plane-parallel electrodes. Thus, Simmons' [4] form of the electron tunneling equations may be employed for the tunneling component of current density. This enables the calculations of the electron tunneling current density to be performed as a function of thickness of the insulating film, s, the metal-insulator barrier height (work function), ϕ, and the applied potential, V.

Assuming a rectangular barrier and neglecting image force, the tunneling current density can be determined from the following where three regions of operation are defined according to the magnitude of the applied voltage.

(a) For V = 0

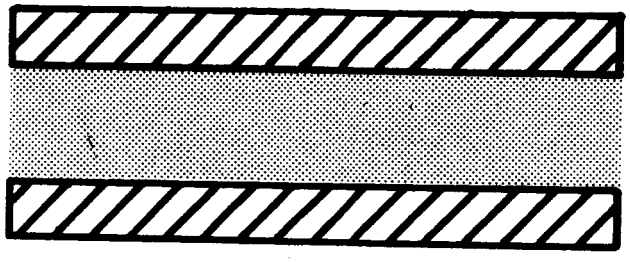

FIGURE 1A

PARALLEL ELECTRODE

MODEL

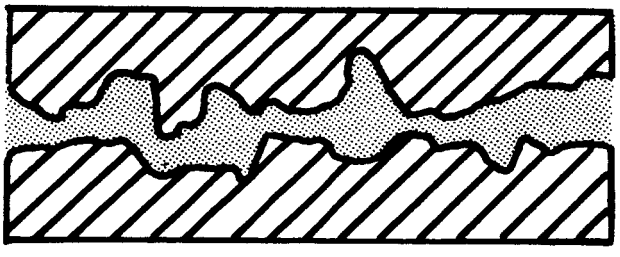

FIGURE 1B

NON IDEAL MODEL

$$J_T = \left[\frac{(2me\phi)^{1/2}}{s} \left(\frac{e}{h}\right)^2 V \right] \exp\left[-(4\pi s/h)(2me\phi)^{1/2}\right]$$

$$= 1.57 \times 10^{10} \phi^{1/2} \left(\frac{V}{s}\right) \exp\left[-0.5125\, s\phi^{1/2}\right] \qquad (1)$$

This corresponds to the Sommerfeld-Bethe [2] result for low voltages.

(b) For $0 < V < \phi$

$$J_T = \left(\frac{e}{2\pi h s^2}\right) \left\{ \left(e\phi - \frac{eV}{2}\right) \exp\left[-\frac{4\pi s}{h}(2m)^{1/2}\left(e\phi - \frac{eV}{2}\right)^{1/2}\right] \right.$$

$$\left. - \left(e\phi + \frac{eV}{2}\right) \exp\left[-\frac{4\pi s}{h}(2m)^{1/2}\left(e\phi + \frac{eV}{2}\right)^{1/2}\right] \right\}$$

$$= \left(\frac{6.2 \times 10^{10}}{s^2}\right) \left\{ \left(\phi - \frac{V}{2}\right) \exp\left[-0.5125s\left(\phi - \frac{V}{2}\right)^{1/2}\right] \right.$$

$$\left. - \left(\phi + \frac{V}{2}\right) \exp\left[-0.5125s\left(\phi + \frac{V}{2}\right)^{1/2}\right] \right\} \qquad (2)$$

which is due to Holm with the exception of an omitted term which Simmons showed was of questionable validity.

(c) For $V > \phi$

$$J_T = \frac{2.2e^2E^2}{8\pi h\phi} \left\{ \exp \left[- \frac{8\pi}{2.96\, heE} (2m)^{1/2}(e\phi)^{3/2} \right] \right.$$

$$\left. - \left(1 + \frac{2V}{\phi} \right) \exp \left[- \frac{8\pi}{2.96\, heE} (2m)^{1/2}(e\phi)^{3/2}\left(1 + \frac{2V}{\phi}\right)^{1/2} \right] \right\}$$

$$= 3.38 \times 10^{10} \frac{E^2}{\phi} \left\{ \exp \left[- 0.345 \frac{\phi^{3/2}}{E} \right] \right.$$

$$\left. - \left(1 + \frac{2V}{\phi}\right) \exp \left[- 0.345 \frac{\phi^{3/2}}{E} \left(1 + \frac{2V}{\phi} \right)^{1/2} \right] \right\} \qquad (3)$$

where $E = V/s$ is the electronic field strength in the insulator. The first term of Equation (3) is the well-known Fowler-Nordheim [8] equation with the exception of a slight modification introduced by Simmons. In the region of interest the second term in this equation is negligible.

For numerical evaluations of the constants an effective electron mass of 1/4 of the free electron mass was assumed because it is generally accepted that this will produce a better correlation between theoretical and experimental results [6], [7]. To agree with the notation used in the literature, the units in the above equation are expressed in J_T [amperes/cm^2], ϕ [volts], and s [angstrom units].

The presence of image charge appearing within the conducting surface reduces the area of the potential barrier by rounding off the corners and reducing the thickness.

To include the effect of image charge on tunneling Simmons [4] has shown that the following substitutions should be made:

(a) For $V \simeq 0$ substitute ϕ_L for ϕ_o and Δs for s in Equation (1) where

$$\phi_L = \phi_o = \left[\frac{5.75}{K(s_2 - s_1)}\right] \ln \left[\frac{s_2 (s - s_1)}{s_1 (s - s_2)}\right] \quad (4)$$

where K is the relative dielectric constant of the film, ϕ_L, the natural barrier height and Δs is the effective thickness of the insulating film for electron tunneling. The effective edges of the barrier are indicated by s_1 and s_2 in Figure 2 and

$$\Delta s = s_2 - s_1$$

$$\text{where } s_1 = \frac{6}{K\phi_o}$$

$$s_2 = s - s_1$$

(b) For $0 < V < \phi_o$ substitute Δs for s and

$$\phi_I = \phi_o - \frac{V}{2} \text{ in Equation (2).}$$

The image reduced barrier height in this case is

$$\phi_I = \phi_o - \left(\frac{V}{2s}\right)(s_1 + s_2) - \left[\frac{5.75}{K(s_2 - s_1)} \ln \frac{s_2 (s - s_1)}{s_1 (s - s_2)}\right] \quad (5)$$

The effective barrier limits are

$$s_1 = \frac{6}{K\phi_o} \text{ and}$$

$$s_2 = s\left[1 - \frac{46}{3\phi_o Ks + 20 - 2VsK}\right] + \frac{6}{K\phi_o}$$

The region for voltage greater than the barrier potential has been neglected in this discussion because it has been shown that the image force has a greater influence on small barriers [4] and because of the extremely high fields required, no true Fowler-Nordheim emission has been observed from experimental methods [5], [6], [9].

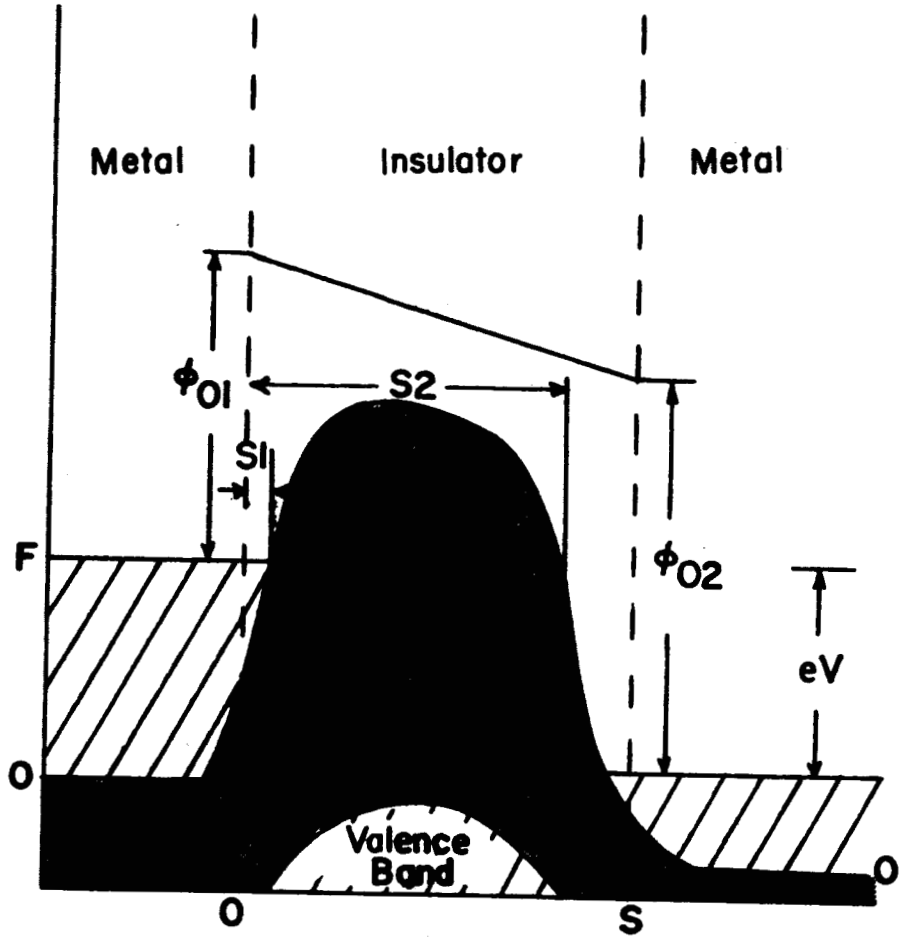

FIGURE 2

BARRIER POTENTIAL MODEL[7]

By the use of Equations (1) through (5) it is possible to express the electron tunneling component of the film current density

$$J_T = f(V, \phi, s) \tag{6}$$

in explicit form. Because of the necessity of using Equations (1) and (2) plus the Fowler-Nordheim equation (if that region is desired), the analysis of laboratory data is greatly simplified by making a continuous plot of Equation (6) in terms of Equations (1), (2), and (3). An extensive set of plots has been made with the aid of a computer. A condensed set of this family of curves is shown in Figure 3. If image force is to be included, then these curves are to be interpreted as a family of curves for various values of ϕ_L or ϕ_I and Δs as defined by Equation (4) and (5).

As the thickness of the insulating layer is increased the probability of electrons tunneling through the barrier decreases exponentially with thickness [5]. Electron currents can be established now only if the electrons have sufficient kinetic or thermal energy to overcome the barrier and move in the conduction band of the insulator. This process is identical with that of Schottky enhanced emission into a vacuum [10] and is thus analyzed accordingly. It is necessary, however, because other than a vacuum is being considered, to introduce the value K, which is the relative dielectric constant of the insulating medium.

The expression for Schottky current density [11] is given by

$$J_s = A(1 - \gamma)\, T^2 \exp\left[\frac{e}{kT}\left\{-\phi_L + \left(\frac{eE}{4\pi K \epsilon_o}\right)^{1/2}\right\}\right] \tag{7}$$

where A is the Richardson-Dushman coefficient,

$$A = \frac{4\pi\, mek^2}{h^3}$$

and has the value 30.1 amp/ cm^2/ $(°K)^2$ when an effective mass of one-fourth the electron rest mass is used. The electron reflection coefficient is γ and E is the electric field strength in volts per centimeter.

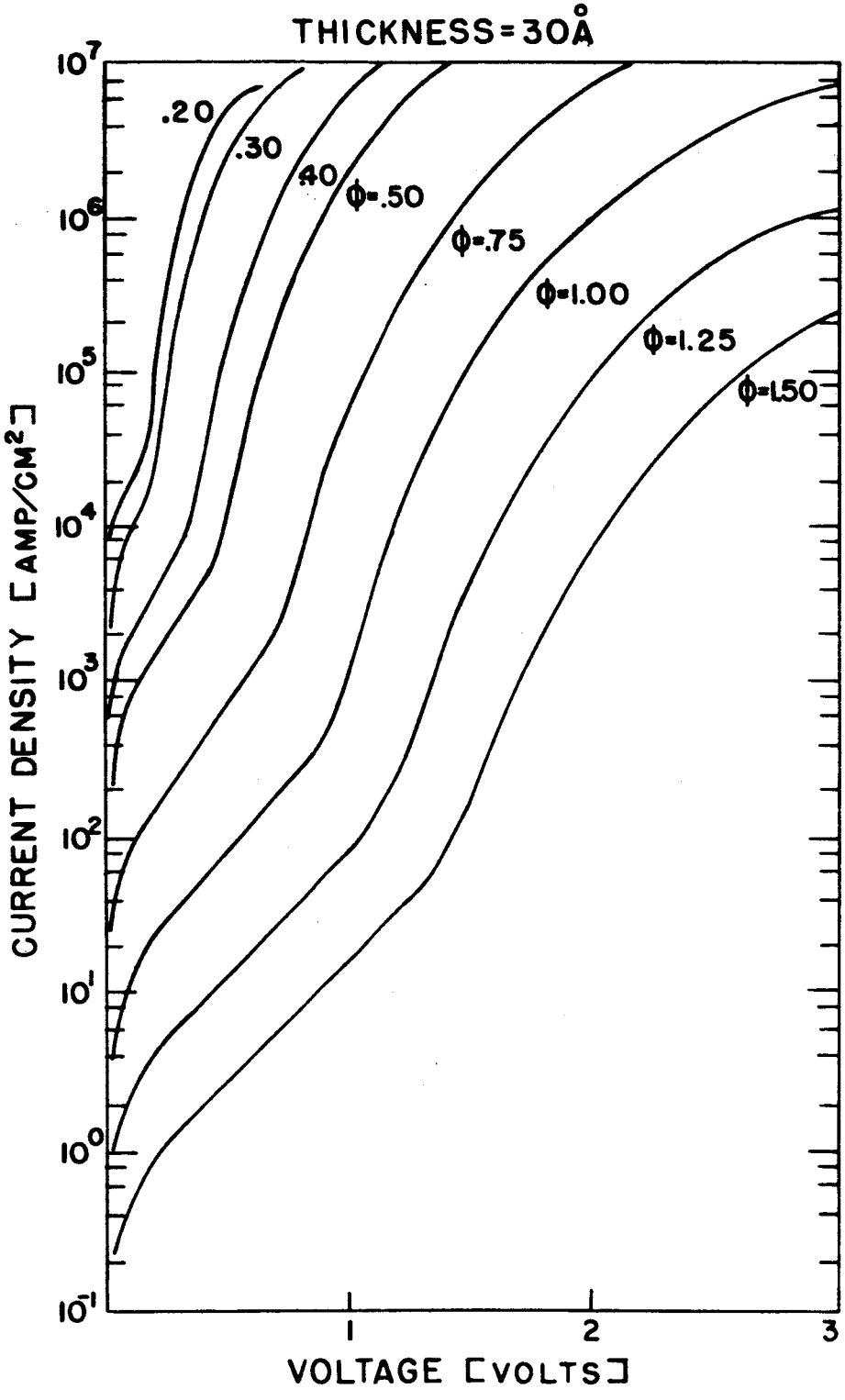

FIGURE 3-1
THEORETICAL TUNNELING CURVES

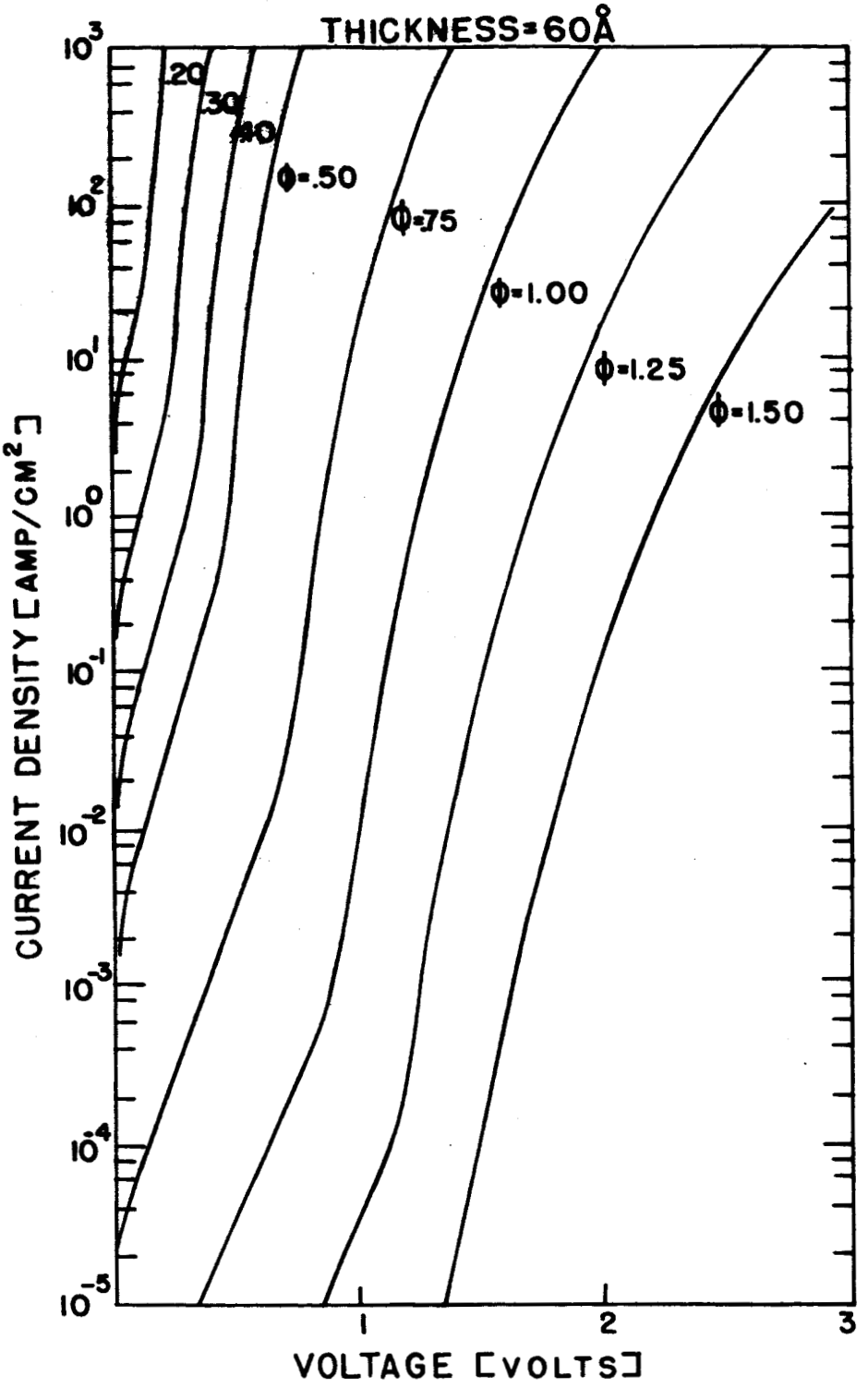

FIGURE 3-2

THEORETICAL TUNNELING CURVES

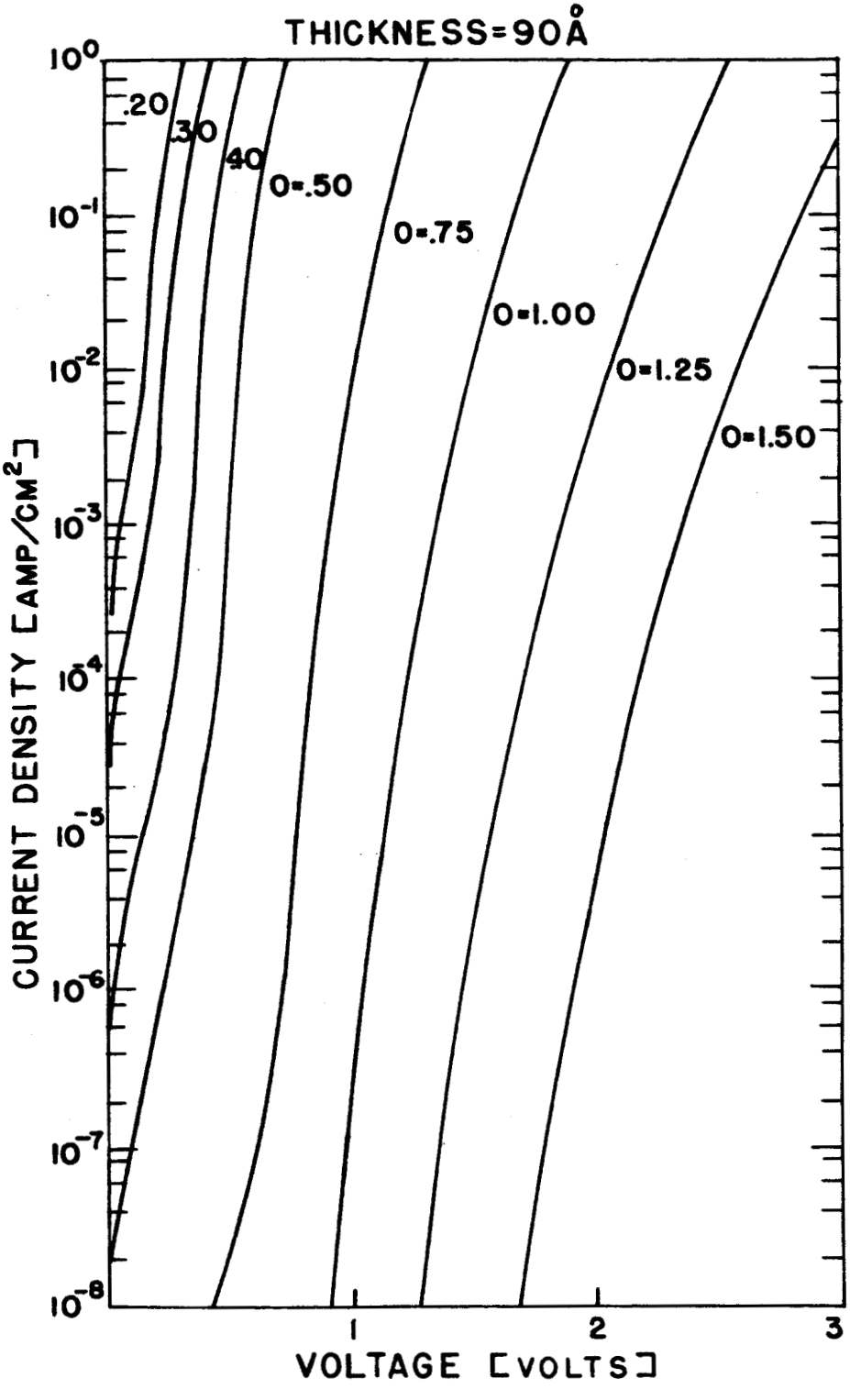

FIGURE 3-3
THEORETICAL TUNNELING CURVES

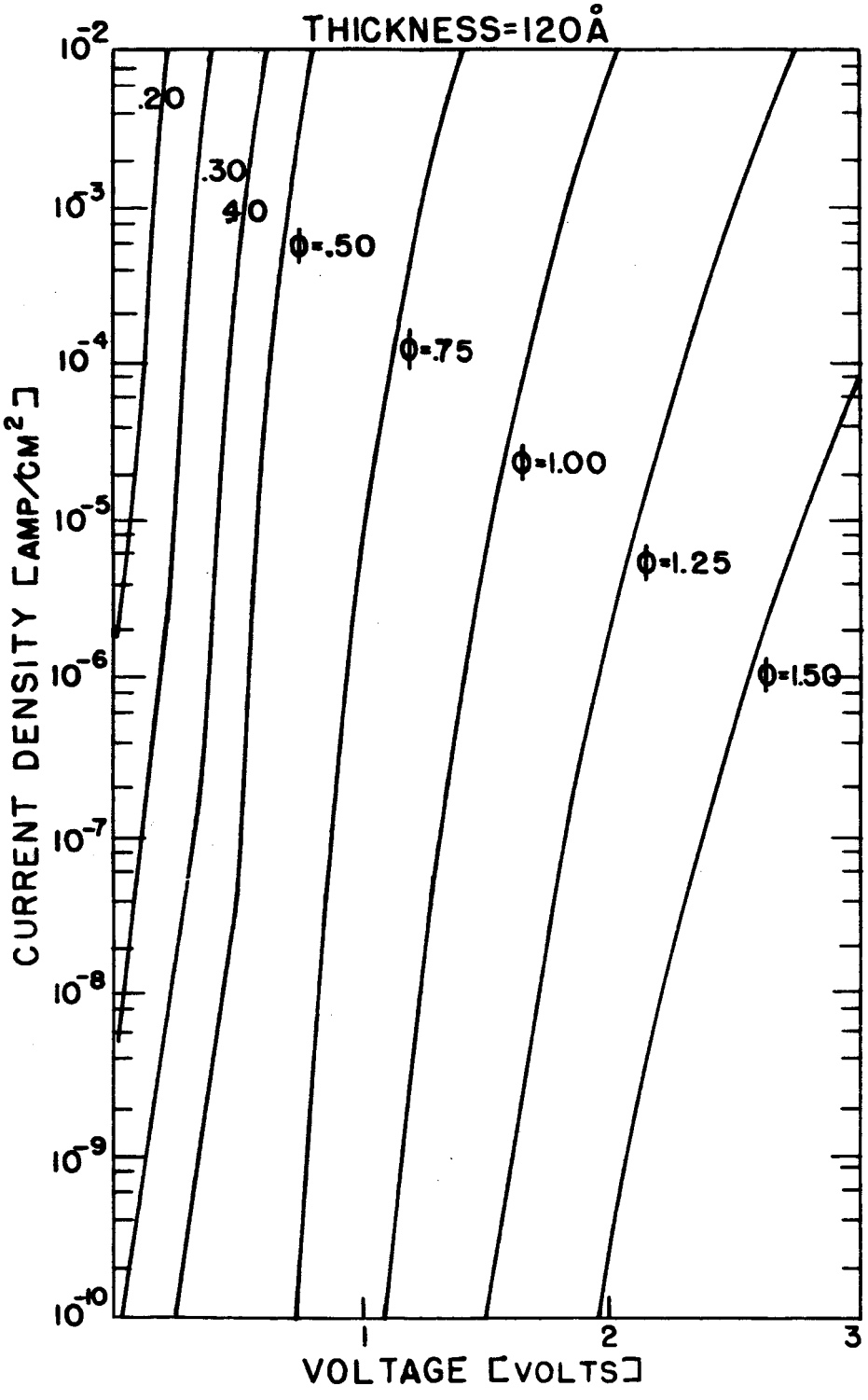

FIGURE 3-4
THEORETICAL TUNNELING CURVES

Explicit analytical expressions for the tunneling and Schottky components of the film current density are presented throughout the literature.

Schottky emission can be characterized by its dependence on temperature while tunneling currents should be completely independent of temperature effects. In thinner films, where Schottky emission predominates at higher temperatures, tunneling may be the electron transport mechanism in the low temperature range. These two components of current can be identified experimentally by plotting $\log_{10} I/T^2$ as a function of $1000/T$. Figure 4 shows this behavior of the current with temperature at constant voltage where Schottky emission over the barrier should be a straight line with negative slope while pure tunneling should have a positive slope of 2T.

The slope of the high temperature portion of Figure 4 is given by

$$.434 \times 10^{-3} c = - \frac{e\phi_L}{k} + 4.4 \left(\frac{E}{K}\right)^{1/2} \qquad (8)$$

This follows from Equation 7 because

$$\log_{10} \frac{I}{T^2} = \log_{10} \langle aA \rangle (1 - \gamma) + 0.434 \times 10^{-3} c \frac{1000}{T} \qquad (9)$$

where a is the area of the device in cm^2. It is possible to evaluate s, E, and ϕ_L from the simultaneous solution of Equation (8) for data determined from Figure 4 for different applied voltages. Therefore:

$$0.434 \times 10^{-3} c_1 = - \frac{e\phi_L}{k} + 4.4 \left(\frac{E_1}{K}\right)^{1/2} \qquad (10a)$$

$$0.434 \times 10^{-3} c_2 = - \frac{e\phi_L}{k} + 4.4 \left(\frac{E_2}{K}\right)^{1/2} \qquad (10b)$$

Substracting Equation (10b) from Equation (10a) yields

$$0.434 \times 10^{-3} (c_1 - c_2) = \frac{4.4 \left(E_1^{1/2} - E_2^{1/2}\right)}{K^{1/2}} \qquad (11)$$

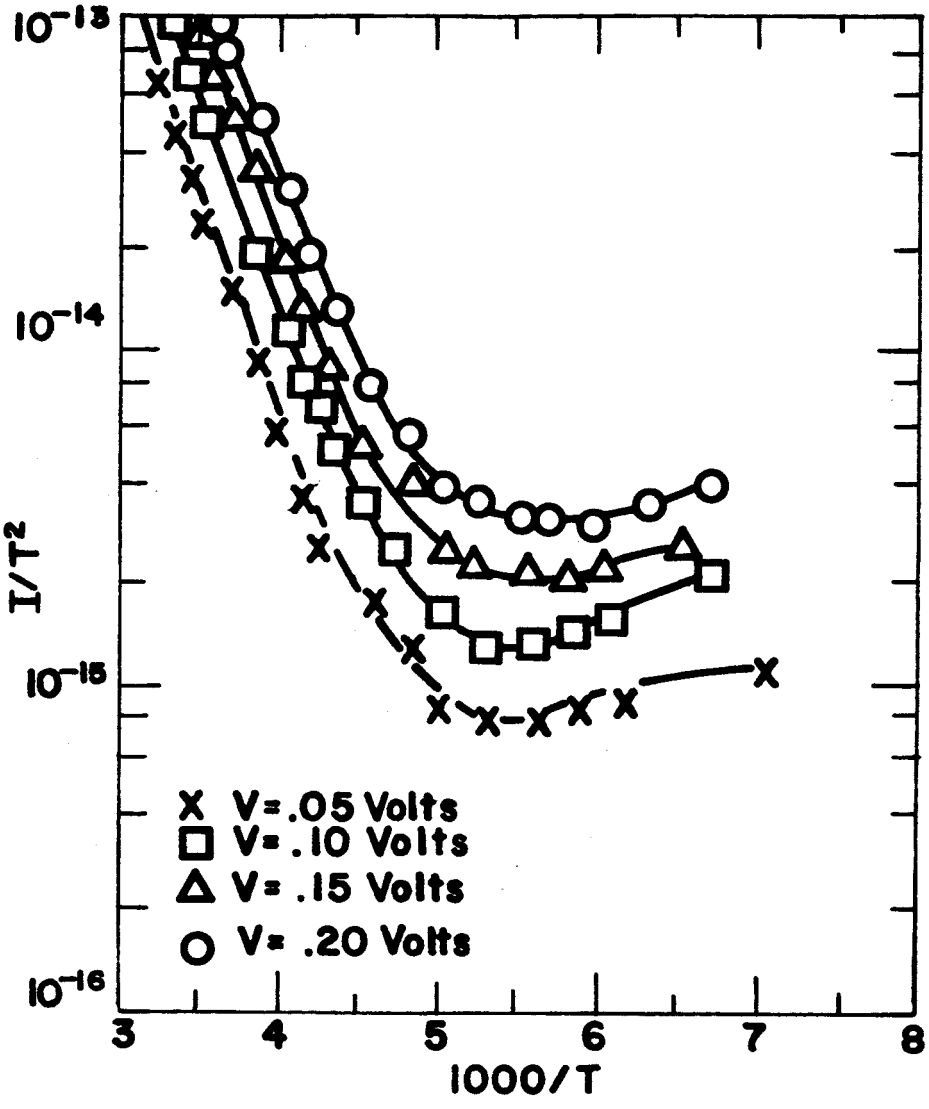

FIGURE 4

VARIATION OF CURRENT WITH TEMPERATURE

but

$$V_2 = nV_1$$

where n is a constant and since the area is assumed to be independent of voltage

$$E_2 = nE_1. \tag{12}$$

Substituting Equation 12 in Equation 11 and rearranging terms yields

$$0.434 \times 10^{-3} (c_1 - c_2) = 4.4 (1 - n^{1/2}) \left(\frac{E_1}{K} \right)^{1/2} \tag{13}$$

which can readily be solved for E_1.
Thus

$$E_1 = \left[\frac{0.434 \times 10^{-3}}{4.4} \quad \frac{(c_1 - c_2)}{(1 - n^{1/2})} \right]^2 K \tag{14}$$

and

$$\phi_L = \frac{k}{e} \left[4.4 \left(\frac{E_1}{K} \right)^{1/2} - 0.434 \times 10^{-3} c_1 \right] \tag{15}$$

$$s = \frac{V}{E_1} \tag{16}$$

The rectangular barrier potential, ϕ_o, may be evaluated by means of Equation (4), which is transcendental in terms of this quantity, using the values of ϕ_L and s determined from Equations (8) through (16).

Based upon the nonideal film structure shown in Figure 1B, the effective electrode area for tunneling is assumed to be the same as that for the Schottky current density. In terms of Equation (7)

$$a = \frac{I_s}{J_s} = \frac{I_s}{A(1 - \gamma)T^2 \exp(c/T)} \tag{17}$$

where I_s, as a function of temperature, is any point selected from the high temperature range of Figure 4.

Figure 5 contains a plot ϕ_I as a function of $(E) = \frac{V}{\Delta s}$ from Equation 6 for one value of V and various values of Δs where the information is taken from Figure 3 and is based upon the tunneling current measured at low temperatures and a computed value of effective emission area, a, based upon an assumed value of γ. Figure 5 also contains a plot of ϕ_I determined from Equation (5), which, using the fact that

$$\Delta s = s_2 - s_1$$

can be rearranged to yield

$$\phi_I = \phi_L - \frac{V}{2s}[\Delta s + 2s_1] \tag{18}$$

The intersection of these two plots yields ϕ_I and Δs thereby, allowing the evaluation of s_2.

It should be noted that evaluation of ϕ_I and Δs depends upon observed tunneling data at liquid nitrogen temperature. As the thickness of the insulator increases, only a small component of tunnel current superimposed on the thermonic current may be observed or the tunneling may disappear entirely.

Films of preselected thickness and high quality were used [12]. The films were deposited on carefully cleaned glass substrates at a pressure of 1×10^{-8} mm Hg (Torr) from molecular beams which were produced by the evaporation of selected materials from electronically heated crucibles [13].

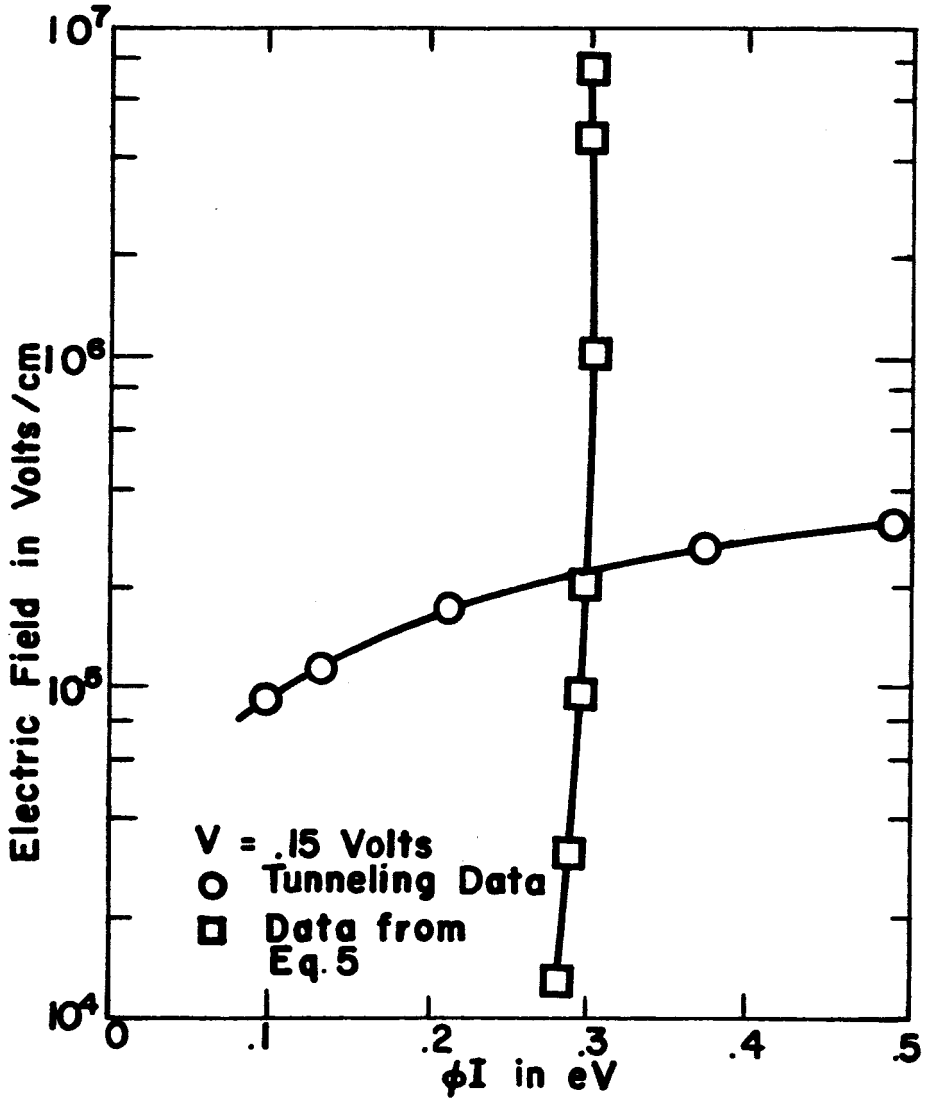

FIGURE 5

PLOT FOR IMAGE BARRIER DETERMINATION

All of the films investigated were of the metal-insulator-metal structure using silicon monoxide as the insulator. The silicon monoxide was evaporated from a newly developed SiO sublimation source [14] machined from reactor grade carbon and suitable for electron bombardment heating. The design was such as to provide the desired molecular beam of SiO molecules while emission of SiO particles was prevented. A deposition rate of 4.2 angstroms per second at a power of about 190 watts was determined by comparing run time against film thickness. Multiple beam interferometer measurements were used to determine film thickness. A calibration curve for SiO is shown in Figure 6.

The principal metal used for the electrodes was gold although silver, lead, and various combinations of the three were investigated. It was found to be advantageous (because of the increased initial charge capacity) to use machined carbon crucibles for the metal vapor sources. However, for gold it was necessary to use dimpled boats of tantalum because of the excessive power required to obtain emission from a carbon boat.

A photo etched stainless steel mask mounted on the linear feedthrough allowed the desired pattern of the multimaterial thin film devices to be obtained. Figure 7 shows the geometric configuration of the films tested. There are five devices per film each with an active area of approximately 0.355 mm^2.

In producing the active device a step was formed when the bottom electrode was deposited onto the glass substrate. Because of the high field concentrations present along the edge of this step, the thin insulating film between the two electrodes was found to be inadequate in preventing electrical breakdown. Therefore, it was necessary to deposit an additional layer of SiO approximately 2500 Å thick along the edges of the bottom electrode (see Figure 7).

It was discovered for the thinner films used that the relative thickness of the metal electrodes became more critical. In order to prevent breakdown along the metal-insulator interface, the thickness of the bottom electrode was not allowed to exceed 600 Å. Best results were obtained when the top

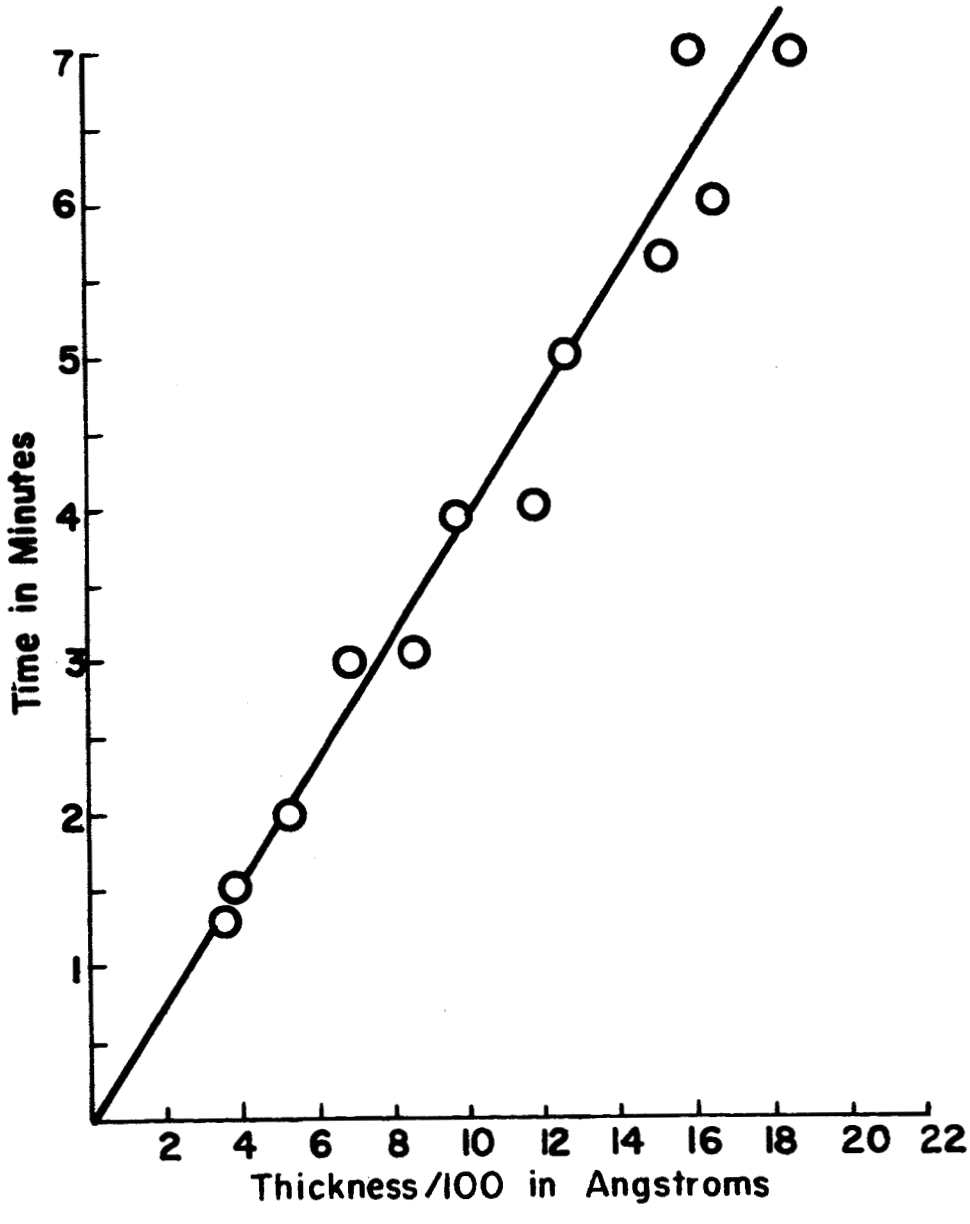

FIGURE 6

SiO CALIBRATION CURVE

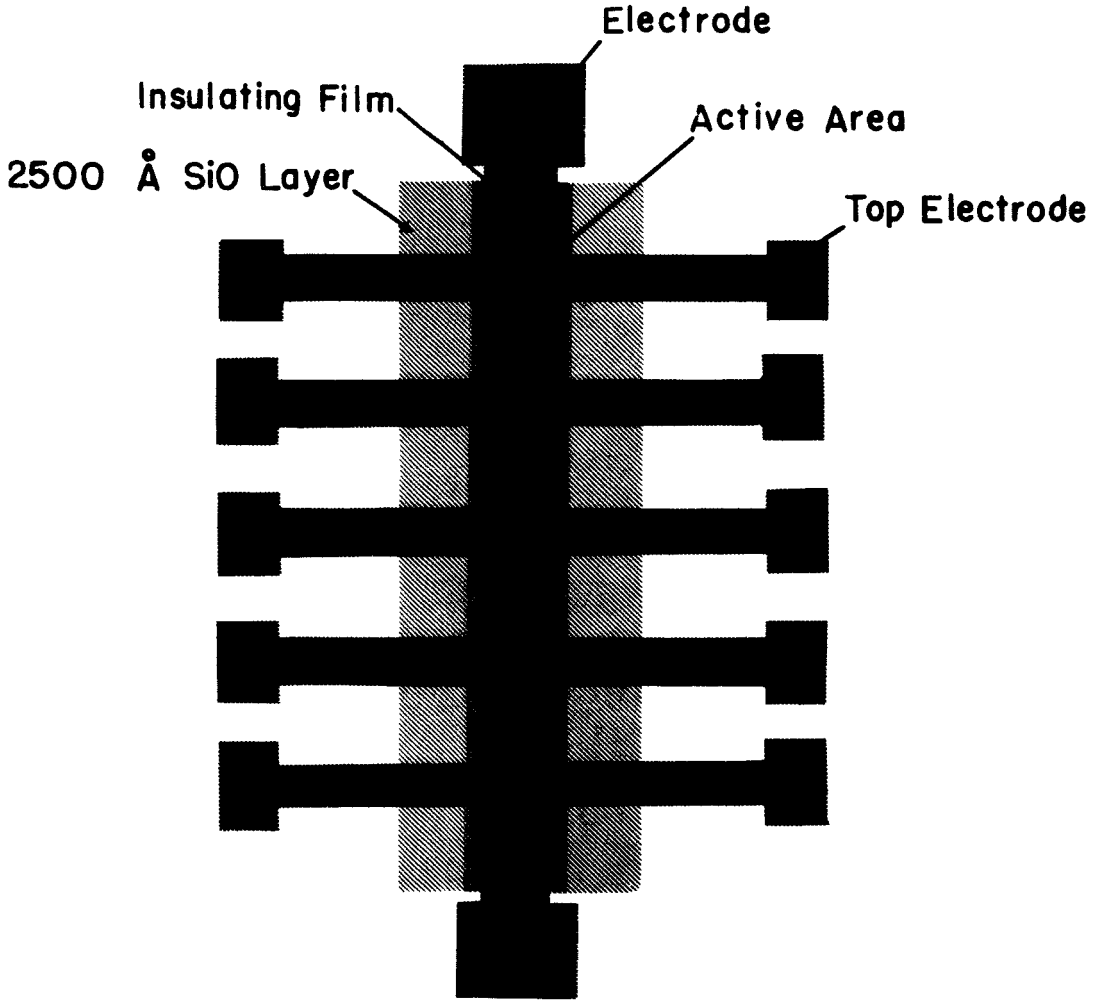

FIGURE 7

DEVICE CONFIGURATION

electrode was approximately 1000 Å thick. Also, the cleanness of the substrate prior to evaporation was determined to be an important factor in obtaining repeatable results.

Indium was used to make electrical contact because of its ability to adhere to glass. Due to their flexibility and high conductivity, gold leads were used.

From the methods discussed previously various thin film structure parameters were determined. All theoretical and transcendental equation solutions were carried out with the aid of a Burroughs B5500 digital computer.

Numerous films of the Au-SiO-Au structure, with a variety of thicknesses (150-750 Å), were tested to determine their temperature dependence. At liquid nitrogen temperature most films tested exhibited almost perfect tunneling characteristics as determined by the independence of current with temperature, while at room temperature Schottky emission was the chief transport mechanism. The transition between the two was observed to occur near 235°K where both components of current had approximately the same magnitude.

Figure 8 shows the same data as that shown in Figure 4 except the straight line Schottky approximations have been extended until an intersection of the $\log_{10}(I/T^2)$ axis was obtained. These are indicated by the broken lines. From Equation (9) it can be seen that on a $\log_{10}(I/T^2)$ vs. $1000/T$ plot the value of the ordinate intercept should be independent of the applied voltage because the effective area is not a function of potential. Therefore, an averaging technique was employed to determine this common intercept value and the curves redrawn as indicated by the solid lines in Figure 8. Experimental inaccuracies were considered to be responsible for these deviations.

For the Au-SiO-Au devices tested $<\phi_L>$, the natural barrier potential, was determined to be .32 eV for a dielectric value of 6 [15], [16]. From Equation (4) $<\phi_o>$, the rectangular barrier potential was

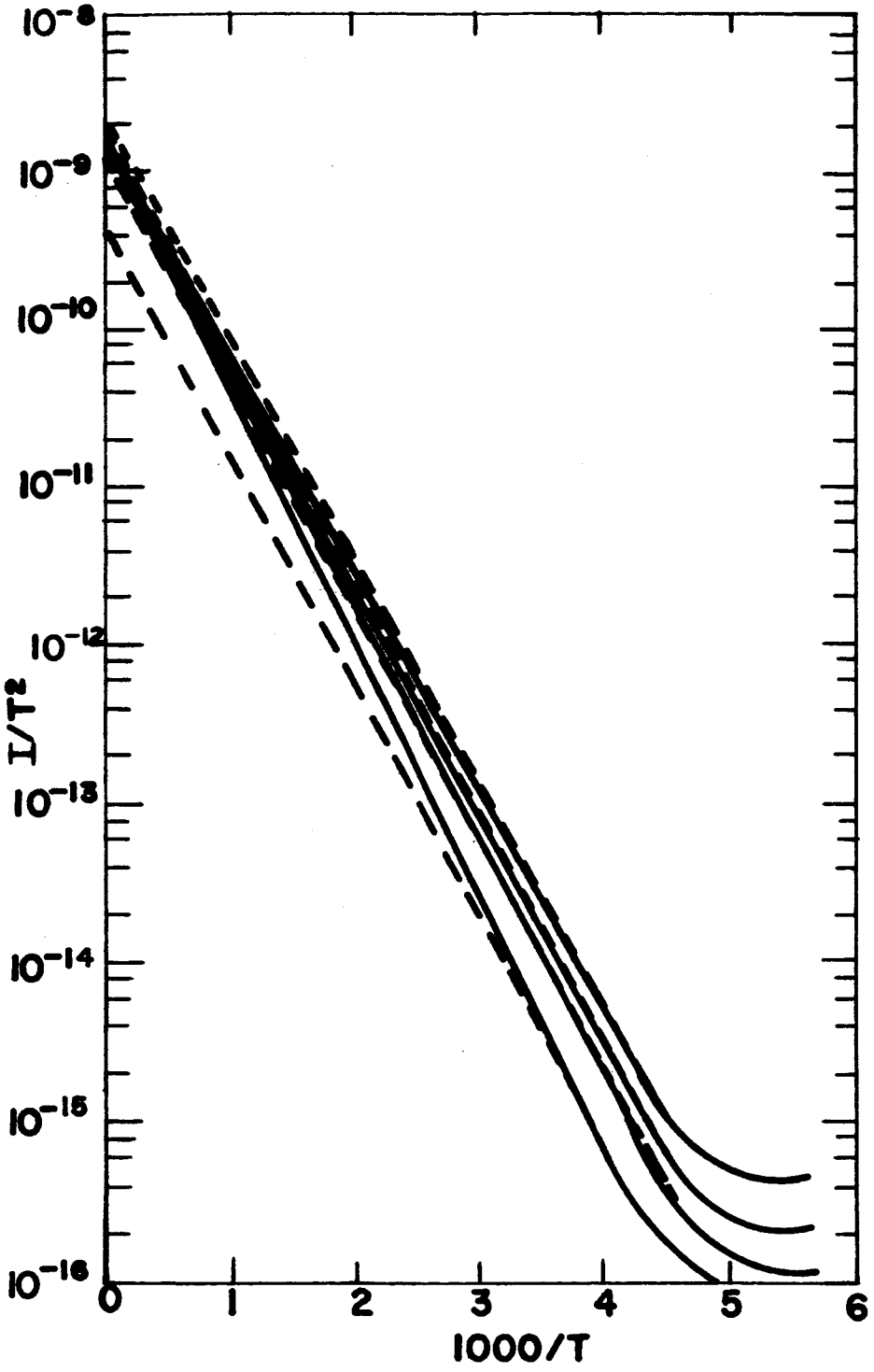

FIGURE 8

VARIATION OF CURRENT WITH TEMPERATURE

SHOWING COMMON INTERCEPT

calculated to be .4 eV. Scales [18] predicted a rectangular barrier potential of .5 eV with a dielectric constant of 4. Using this value, exact agreement was obtained; however, a dielectric strength of 6 is more commonly accepted [16]. From the data shown in Figure 4 $\langle s \rangle$ was determined to be 95 Å. The interferometer thickness was 420 Å thus supporting the model of close electrode approach presented in Figure 1B. Tunneling data was available for this device at liquid nitrogen temperature. From Schottky data the effective area was determined to be $.3 \times 10^{-6}$ of the gross geometrical area. Using Figure 5, Δs and ϕ_I were determined as 60 Å and .3 eV respectively.

Pollack [19] presented current-voltage-temperature data for a Pb-Al_2O_3-Pb film where he determined a natural barrier potential of .64 eV and a measured thickness of 340 Å. Applying the previously described method $\langle \phi_L \rangle$ was determined to be .66 eV. Other parameters determined were $\langle \phi_o \rangle$ of .73 eV and $\langle s \rangle$ of 63 Å. A dielectric value of 12 as employed by Pollack was used in all calculations.

In a similar manner data presented by Standley, et al. [10] for a Ta-Ta_2O_5-Au film was investigated. A value for the natural barrier potential of .63 eV was given for the film which was estimated to have an insulator thickness of 110 Å. From analysis of this data $\langle \phi_L \rangle$ was found to be .66 eV and $\langle \phi_o \rangle$ calculated to be .78 eV. The mean effective film thickness $\langle s \rangle$, was determined to be 22 Å.

It can be seen that almost exact agreement was obtained for the natural barrier potentials from the analysis of data presented in the literature. In each investigation $\langle s \rangle$ was determined to be approximately one-fifth of the interferometer measured thickness. Future investigation is planned to determine if this fact is of any significance.

Variations in the reflection coefficient had little or no effect upon the final result over the range of the experimental data obtained. It is unlikely that a metal-insulator interface would have an appreciably large reflection coefficient, and it has been suggested [7] that a good approximation is to neglect it completely.

In order to verify the tunneling hypothesis, it was necessary to establish that the current-voltage characteristics were independent of temperature. Various experiments were conducted over a temperature range from liquid nitrogen at 73°K to room temperature at 300°K. All samples with an approximate thickness less than 100 Å exhibited no temperature effects thus establishing that tunneling was the only conduction process. As the thickness of the insulator was increased Schottky emission became more apparent and eventually became dominant.

Figure 9 shows the test circuit used in obtaining the d-c voltage-current data. It was discovered that identical information could be obtained using pulse techniques if the pulses were of sufficient length. This has also been verified by others [7]. As predicted from tunneling theory for low voltages, the current was proportional to the voltage, demonstrating an ohmic relationship. As the voltage was increased the current increased exponentially as could be expected from Equation 2. Figure 10 shows these characteristics plotted from experimental data for an Au-SiO-Au sample.

All theories concerning tunneling are based on ideal plane-parallel electrodes assuming uniform thickness whereas the effective surface area for emission may be only a small fraction of the gross geometrical area of the structure as explained in the theory. Various methods have been attempted to alleviate these shortcomings; however, at present the best correlation between experimental and theoretical results appears to exist when one considers plane-parallel electrodes separated by an effective insulator thickness.

For the gold-silicon monoxide tunneling structures, film breakdown occurred for applied potentials of approximately .7 volts. This would tend to indicate that breakdown was occurring at the beginning of the Fowler-Nordheim region or where the work function and applied potential became equal. Breakdown was higher than the work function of .4 eV determined for the rectangular barrier. A possible explanation for this can be that instead of considering the field to be determined by the relationship $E = \frac{V}{s}$,

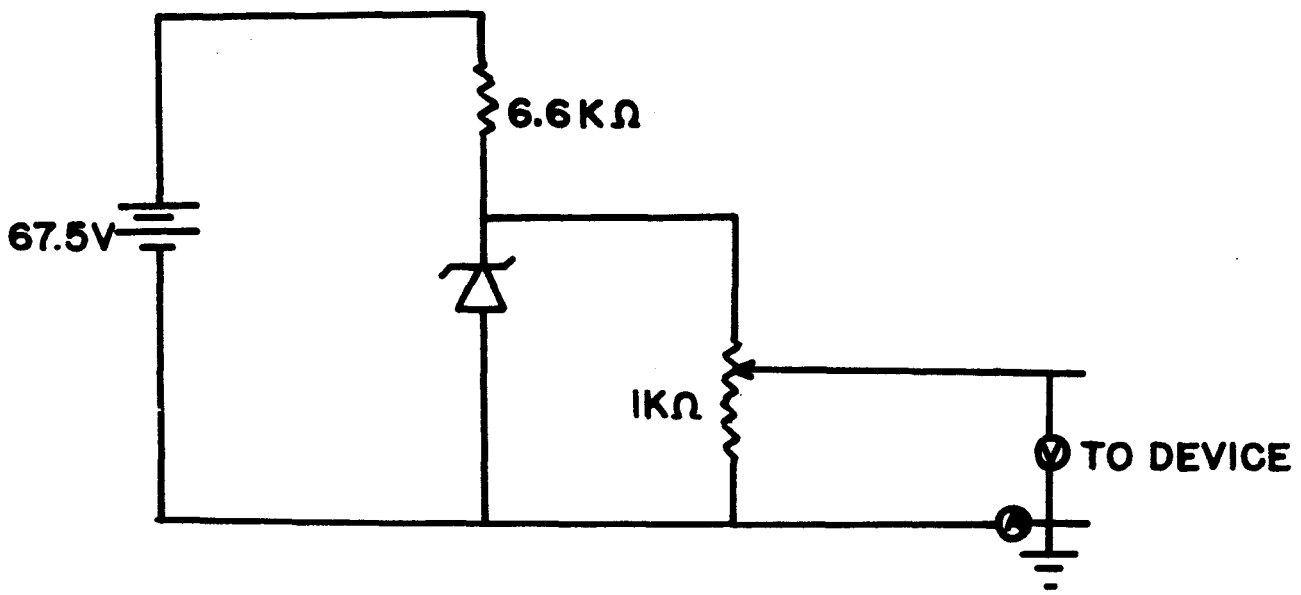

FIGURE 9

DEVICE TEST CIRCUIT

NOTE:

(1) VOLTMETER WAS A MODEL 610B

KEITHLEY ELECTROMETER

(2) AMMETER WAS A MODEL 425 A

HEWLETT PACKARD DC MICRO-VOLT-AMMETER

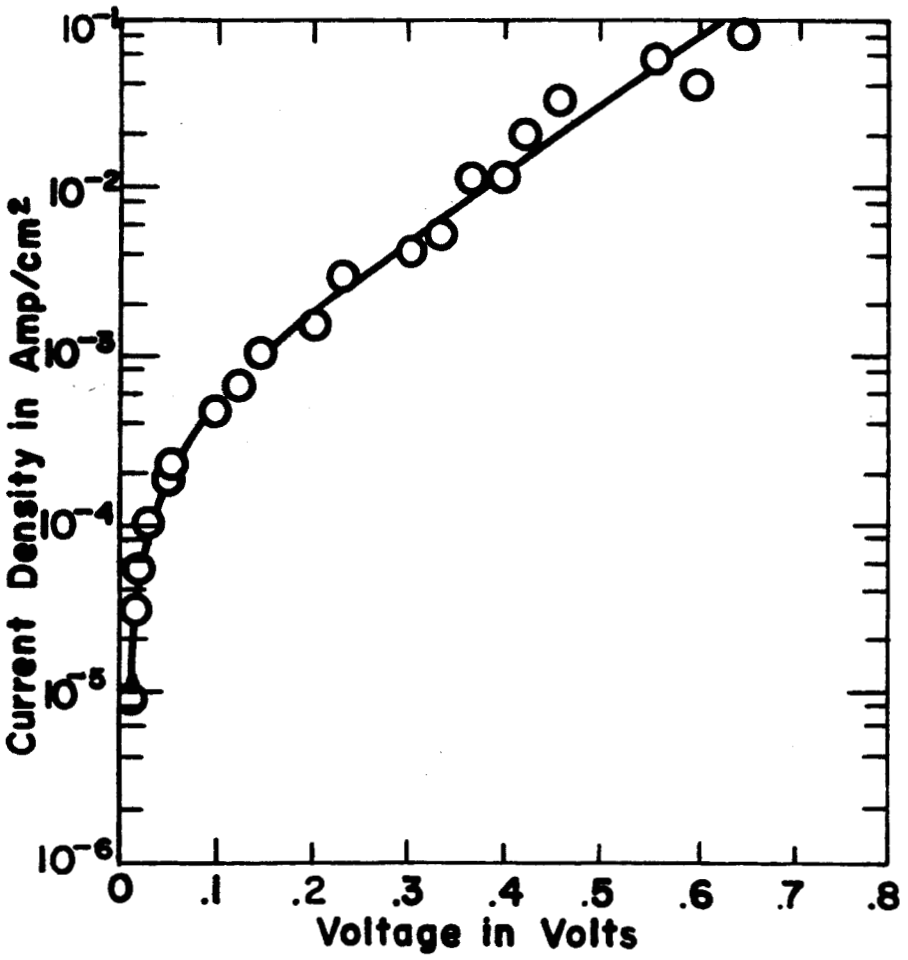

FIGURE 10

EXPERIMENTAL TUNNELING CURVE

high voltage techniques must be employed. Thus:

$$E = \beta V \tag{19}$$

where β is the form factor associated with the negative electrode, must be employed to account for any localized high fields which might exist. Future investigation is planned to determine the extent of variation produced by these localized high fields and to obtain a value for β which would give rise to a more accurate model for tunneling junctions. In obtaining experimental verifications of the ideas presented, several thin film phenomena were observed which are worthy of mention.

I. Observed Switching

For Au-SiO-Au films between 200 and 300 Å thick a switching effect in the direct current-voltage characteristic was repeatedly observed. Figure 11 illustrates this for one sample. Initially as voltage was increased across the device, the current approached an ohmic relationship until a potential of approximately 1.5 volts was applied. The current then dropped two orders of magnitude giving the indication that the I-V characteristics had a region of negative resistance. Maximum peak-to-valley ratios of 300:1 have been reported; however, ratios of approximately 1000:1 were observed here for some cases. It is observed for all samples with this negative resistance region that the measurable current was extremely noisy and highly erratic. No consistency was obtained in the data from sample to sample. Due to the extremely fast switching time it was impossible to obtain any data in the negative resistance region. The repeatability was extremely poor with film destruction often occurring immediately following the switching phenomena.

Hickmott [20] has concluded that the establishment of conductivity and negative resistance in insulating films was due to a "forming process". He stated that this forming of conductivity was dependent on the field in the oxide, on purity of the oxide, on the metals used for electrodes, and on the

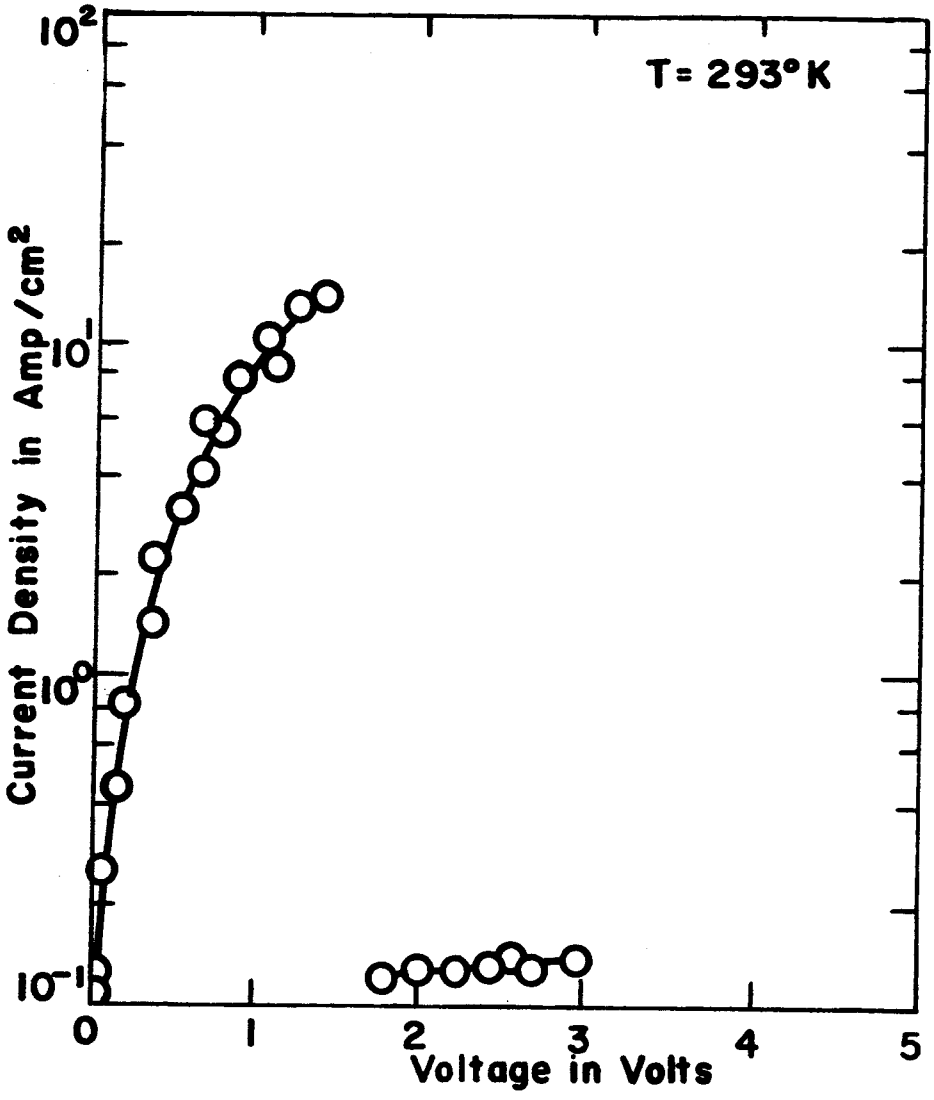

FIGURE 11

NEGATIVE SWITCHING

environment. Thus, due to the impurities present such as Si and SiO_2 and because of the structure of the oxide layer, negative resistance was detected in films of certain critical thicknesses.

The circuit shown in Figure 12 was used to obtain current voltage relationships for films exhibiting this switching effect. A 1000 cycle signal was applied and the effects of varying the amplitude were observed on an oscilloscope screen. Figure 13 shows a sample of the results obtained. This film had an initial low conductivity as shown by the data in Table I. As the voltage was increased, the conductivity, approximated by the slope at zero voltage, increased until a maximum occurred at 2 volts. Further voltage increases beyond this point resulted in a reduction of conductivity. By observing the nature of the traces shown in Figure 13 it can be deduced that the sample was a nonlinear device. These results were similar to those observed by Hickmott [21] for $Al-Al_2O_3-Al$ structures but as this switching phenomenon was not the primary objective of this research, further investigation of its causes and effects has been set aside for future research.

II. Effect of Electrodes on the J-V Characteristics

For devices having electrodes of the same material it was found that the J-V characteristics were independent of the polarity of the applied voltage. Thus, it can be concluded that the metal-insulator potential barrier was symmetrical.

Simmons [22] has extended the theory of tunneling to include devices having electrodes of different materials and work functions. He proposed that in these devices, because of the difference in work functions of the electrodes, there exists an intrinsic field which produced an asymmetric potential barrier. From this it can be concluded that the J-V characteristics are polarity-dependent with the greater current existing for low voltages when the electrode of lower work function is positively biased. At higher voltages a larger current is obtained when the electrode of lower work

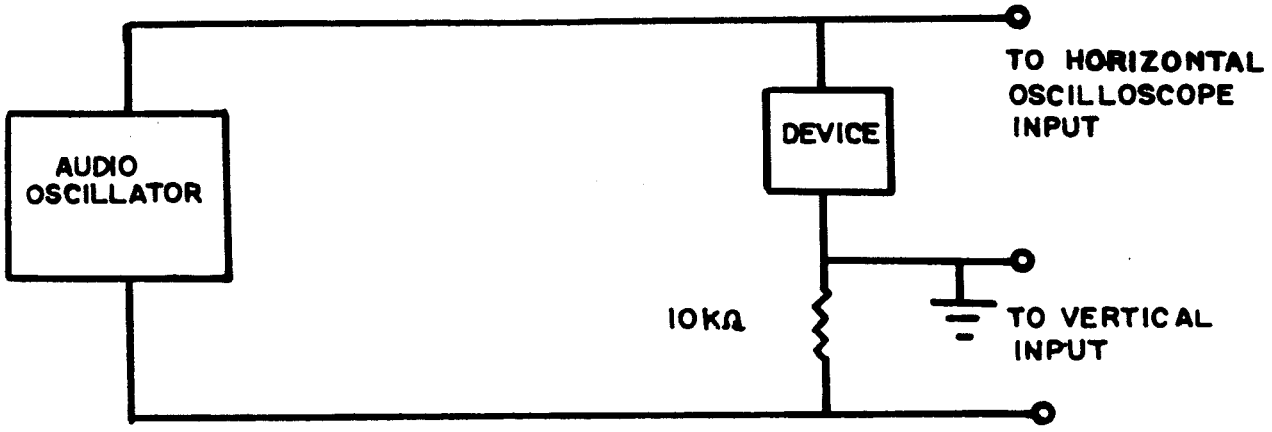

FIGURE 12
TEST CIRCUIT FOR A.C. SWITCHING

TABLE I
A.C. SWITCHING DATA*

FILM CONDUCTANCE (MHOS X 10^{-3})	MAXIMUM IKC VOLTAGE
0.91	0.2
3.75	2.0
2.50	2.2
1.25	3.8
0.20	9.0

*. SEE FIGURE 13

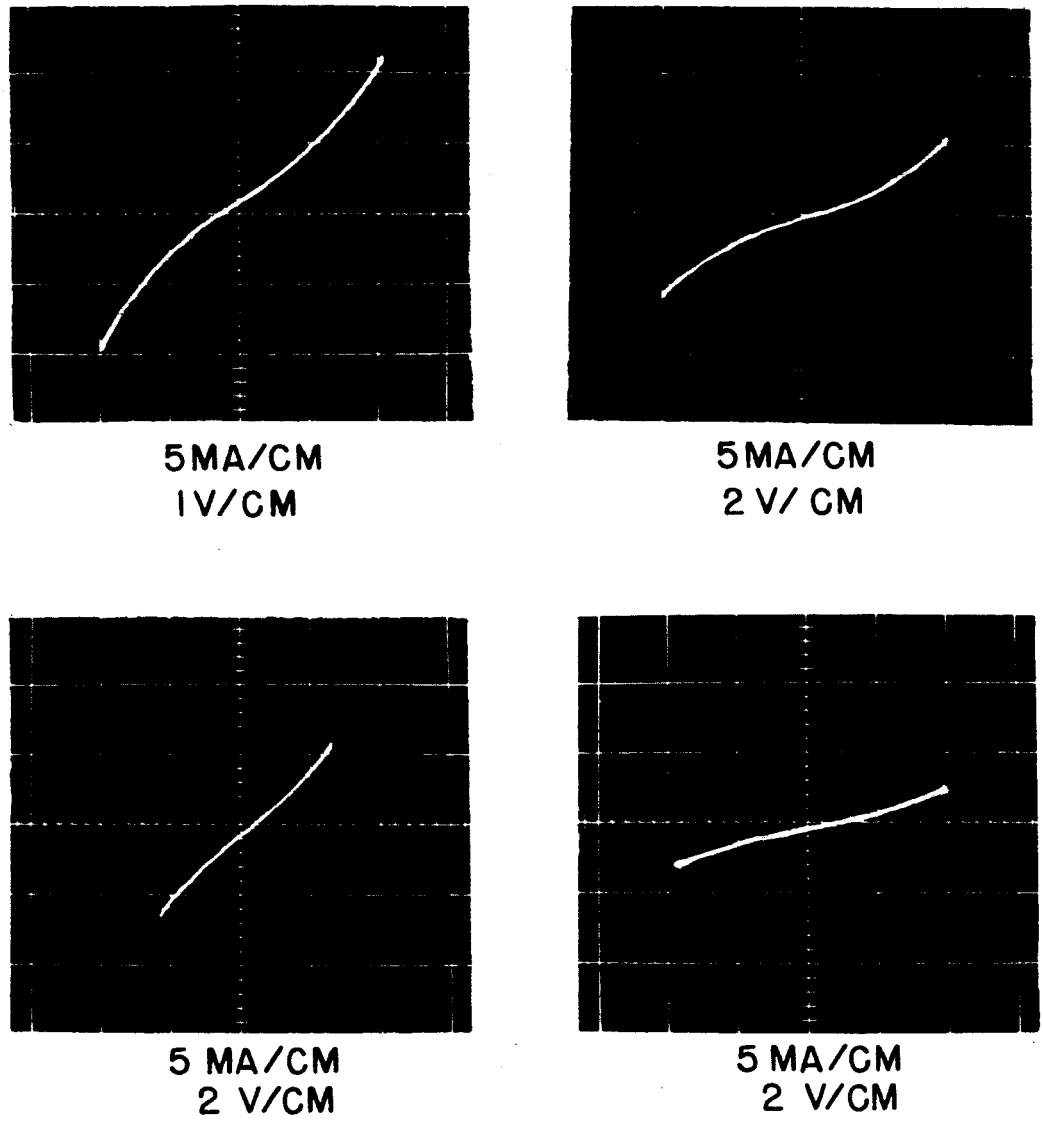

FIGURE 13

1000 CYCLE CURRENT-VOLTAGE
CHARACTERISTICS OF A SiO FILM
(ABCISSA IS VOLTAGE; ORDINATE IS CURRENT)

function is negatively biased. Figure 14 illustrates this for a Au-SiO-Pb film and thus from Simmons' explanation it can be concluded that the barrier potential for lead is greater than that for gold. Silver was also used as the counterelectrode but because of randomness of the results no conclusions could be drawn.

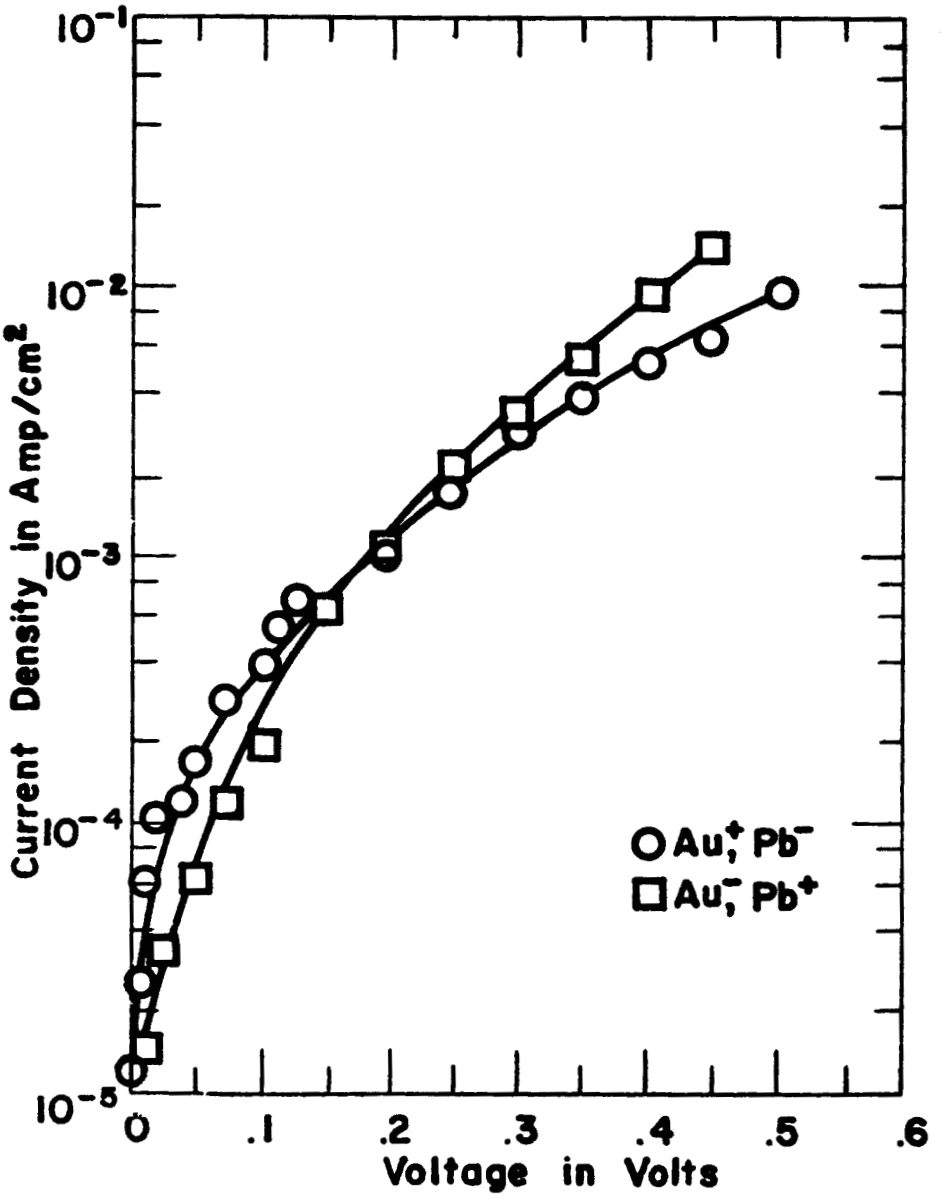

FIGURE 14

TUNNEL EFFECT BETWEEN DISSIMILAR ELECTRODES

SECTION IV
FUTURE RESEARCH

We are currently concluding a theoretical and experimental study of electronic conducitivity in polycrystalline thin films. It is anticipated that the results of this study will permit us to return to the problem of depositing acceptable thin film field effect transistors of the MOS-FET type.

Research on electron tunneling is continuing with the intention of divising several control type devices of an active nature. Included in this research will be a continuation of the metallic whisker cathode idea.

Some high temperature device investigation is being initiated. It is felt that certain thin film devices may be better suited to high temperature operation as contrasted to the usual room temperature or cryogenic temperature ranges so commonly under investigation today.

BIBLIOGRAPHY

1. J. Frenkel, Phys. Rev. 36, 1604 (1930).

2. A. Sommerfeld and H. Bethe, Handbuch Der Physik (Edited by Geiger and Scheel), Vol. xxiv/ 2, p. 450, Springer, Berlin (1933).

3. R. Holm, J. Appl. Phys. 22, 569 (1951).

4. J. G. Simmons, J. Appl. Phys. 34, 1793 (1963).

5. J. C. Fisher and I. Gaiver, J. Appl. Phys. 32, 172 (1962).

6. R. Stratton, J. Phys. Chem. Solids 23, 1177 (1962).

7. D. Meyerhofer and S. A. Ochs, J. Appl. Phys. 34, 2537 (1963).

8. R. H. Fowler and L. Nordheim, Proc. Roy. Soo. (London) 119, 173 (1938).

9. D. P. Seraphim, Thin Films (American Society for Metals, Metals Park, Ohio, 1963), p. 143.

10. C. L. Standley and L. I. Maissel, J. Appl. Phys. 35, 1530 (1964).

11. R. L. Ramey, Physical Electronics (Wadsworth Publishing Company, Inc., Belmont, California, 1961), p. 106.

12. R. L. Ramey, RLES Report No. EE-4012-101-64U, (Univeristy of Virginia, Charlottesville, Virginia), January 1964.

13. R. L. Ramey, R. B. Brownell, W. D. McLennan, and E. J. White, Rev. Sci. Instr. 35, 1147 (1964).

14. E. J. White, (private communication).

15. F. W. Schenkel, Electronics 67, 70 (January 25, 1965).

16. W. B. Nowak and J. J. O' Connor, IEEE Trans. (Parts, Mat. and Pack.)1, S - 186 (1965).

17. P. R. Emtage and W. Tantraporn, Phy. Rev. Let. 8-7, 267 (1962).

18. J. L. Scales, NASA Report 1162, (1963).

19. S. R. Pollack, J. Appl. Phys. 34, 877 (1963).

20. T. W. Hickmott, J. Appl. Phys. 33, 2669 (1962).

21. T. W. Hickmott, J. Appl. Phys. 35, 2118 (1964).

22. J. G. Simmons, J. Appl. Phys. 34, 2581 (1963).

DISTRIBUTION LIST

Copy No.	
1 - 10	Office of Grants and Research Contracts Code CD National Aeronautics and Space Administration Washington, D. C.
11	A. R. Kuhlthau
12	M. G. Foster
13 - 17	R. L. Ramey
18 - 25	RLES Files